

WOLLASTONITE : A REACTIVE MINERAL TO ALKALI-AGGREGATE REACTION

P. Rémy and M. Brouxel

DUNE Travaux Spéciaux, Centre d'Entreprise et d'Innovation, Campus Universitaire de la Doua, BP 2132, 69603 Villeurbanne Cedex, France

A water tank built along the sea and showing expansion signs was studied in detail. Abundant AAR gels were observed with the polarizing microscope and the scanning electron microprobe. The chemical composition of the gel was determined using an electron microprobe and the EDXA coupled with the SEM. Important variations, related to the environment conditions, were observed: for example, gels coming from concrete sampled in parts facing the sea presents higher sodium contents than gels coming from concrete sampled in parts not facing the sea. Most of the gel veins are coming from metamorphic limestones aggregates and are intimately associated with wollastonite ( $\text{CaSiO}_3$ ). This silicate mineral is likely reactive to AAR and do present moreover a chemical composition very close to the gel composition.

INTRODUCTION

The numerous studies conducted over many years on alkali-aggregate reactions (AAR) enlighten the wide range of reactive rocks and minerals (e.g. Coull (1)). Various forms of silica (opal, chalcedony, tridymite, cristobalite, volcanic glass) and various forms of quartz (crypto-crystalline, micro-crystalline ...) or deformed quartz crystals (strained, fractured, granulated ...) have been reported as very reactive to AAR. Reactions involving silicate minerals like feldspar or mica are rarely cited and are the subject of intense debates. Moreover, these minerals are usually considered as providing alkalis rather than silica. AAR involving calcareous aggregates are also sometimes evokated, especially in Canada where metamorphic siliceous limestones aggregates are commonly used (Rogers (2), Fournier and Bérubé (3, 4)).

This paper describes an AAR phenomenon taking place in a concrete made with volcanic and limestones aggregates. Located on the Saint Martin Island (French Antilles), the studied structure, a water tank on the seashore, is the first described example of AAR on a French Antilles island. This is quite astonishing because most of the used aggregates on these islands are of volcanic origin (porphyritic basalts, andesites and dacites). These rocks contain high amounts of volcanic glass which have been described as reactive to the AAR (1). The aim of this paper is to describe the AAR products using a polarizing microscope and a scanning electron microscope (SEM). The relationships between the aggregates and the gel, as well as the chemical composition of the gel will also be presented.

DIAGNOSIS AND SAMPLING

The studied concrete structure, a circular water tank (high = 7.2 m, diameter = 32 m) was built in 1986 along the seashore on the Saint Martin island (French Antilles). The first degradations were observed in June 1987. A circumferential crack and several vertical cracks appeared. Map-cracking and abundant pops were also recorded. The increasing number of pops over a short period of time (50 to 90% increase in 4 months, after less than a year of service life) indicates that a rapid expansion phenomenon took place. The presence of white exudates on the surface as well as a

higher number of pops in the parts facing the sea suggested that the reservoir was affected by AAR. Accelerated expansion tests were conducted on mortar bars made using aggregates sampled in the concrete tank (24 hours cycles at 120 °C and 2.5 bars). The measured expansions, ranging between 0.08% and 0.15% after 5 cycles, confirm the reactivity of these aggregates to AAR.

Twelve drilled cores were sampled on the tank; the highest number being collected on the most deteriorated parts which are facing the sea (Figure 1).

### ANALYTICAL PROCEDURES

Being aware that AAR gels were present in the studied concrete, special attention was given to the sample collection and preparation. They were carefully packed in order to preserve their humidity and to prevent carbonation. Moreover, thin-sections were prepared with petroleum as a lubricant to prevent dissolution or alteration of the gels (several authors are using methanol as a lubricant; Durand and Berard (5), Regourd-Moranville (6)). It was therefore possible to observe the same sample, first, with a polarizing microscope, and second, with a SEM. It was also possible to analyze the different phases with an electron microprobe. The comparison of these accurate results with the semi-quantitative analyses obtain with the Energy Dispersive X-Ray Analysis (EDXA) system coupled with the SEM will also be presented.

The electron microprobe analyses have been carried out on the CAMEBAX probe at the "Service Communs d'Analyses" of the University of Nancy I. The analytical procedures followed in this study for the SEM and EDXA analyses are similar to those reported in detail by Brouxel (7) and only a brief outline is given here. The accuracy and reliability of the analyses was determined as follow (7). Fifteen reference samples, obtained from the Geostandards International Working Group "Analytical Standards of Minerals, Ores and Rocks", were melted, and analyzed. The obtained values were then compared with the accepted values of these standards (Govindaraju (8)). This study showed that the sodium and magnesium contents were underestimated respectively by a factor of 3.3 and 1.7, while the potassium content was overestimated by a factor of 0.7. The analytical results were therefore corrected for this analytical bias. This study allowed also an estimation of the accuracy of the EDXA technique : the analytical errors used in this study are :  $\text{SiO}_2 \pm 4\%$  ;  $\text{CaO} \pm 1.1\%$  ;  $\text{Al}_2\text{O}_3 \pm 2.3\%$  ,  $\text{MgO} \pm 1.0\%$  ;  $\text{Na}_2\text{O} \pm 1.2\%$  ;  $\text{FeO} \pm 1.8\%$  ;  $\text{K}_2\text{O} \pm 0.9\%$  . After correction, the EDXA results are, within error, similar to the electron microprobe analyses (7).

### RESULTS

The studied concrete is made of limestones (60 %) and volcanic aggregates. The volcanic rocks are mostly of andesitic composition and contain plagioclase and amphibole phenocrysts. Various types of limestones aggregates are present in this concrete (micritic and bioterritic limestones) but this study will focus on a particular type : metamorphosed limestones. All the gels were found within this type of aggregates or in cracks or veins coming from these aggregates. These limestones, containing wollastonite, were likely formed by high temperature metamorphism at the contact with a volcanic flow. Wollastonite is a common mineral of metamorphosed impure limestones where the silicium is metasomatically introduced (Deer et al (9)). In most of these occurrences, it is the result of the reaction :  $\text{CaCO}_3 + \text{SiO}_2 \longleftrightarrow \text{CaSiO}_3 + \text{CO}_2$  (9).

The petrographic study showed many cracks going through the cement paste but also through some aggregates. Most of the cracks does contain an amorphous gel. Rosette-like gels were also observed but only inside the metamorphic limestones aggregates. An example of the relationships between the gel and the aggregates is described with SEM micrographs (Fig. 2, 3, and 4). Fig. 2 shows a vein filled with gel (dark grey) crossing a metamorphic limestone aggregate. The left part of the vein is made of wollastonite crystals (white crystals) imbedded in calcite matrix (pale gray). Farther to the left (Fig. 3 and 4), the wollastonite crystals are imbedded in a rosette-like gel (black).

The aspect of these gels is not typical : this is related to the fact that these micrographs are in two dimensions (these observations are made on a thin section). It can be seen in Fig. 3 that some gels are formed inside of some wollastonite crystals.

The micro-analyses of these gels are presented in table 1 and 2 together with the analyses of the cement paste and all the minerals observed in this concrete (calcite, wollastonite, plagioclase and amphibole). It can be seen that there is a rather good agreement between the EDXA analyses (E) and the microprobe analyses (M).

The chemical composition of the gel is the following :  $\text{Na}_2\text{O}$  : 0 to 7 %,  $\text{SiO}_2$  : 31 to 74 %,  $\text{K}_2\text{O}$  : 0 to 11 %,  $\text{CaO}$  : 18 to 69 %. Important chemical variations were observed not only between different samples but also within the same sample. The  $\text{SiO}_2$  versus  $\text{CaO}$  diagram is presented in Fig. 5. As already shown by Knudsen and Thaulow (10) and Brouxel (11) there is a negative correlation between  $\text{SiO}_2$  and  $\text{CaO}$ . This correlation, almost parallel, but also very close, to the 100% line indicates that the AAR gels show only a small enrichment in alkali.

The composition of the gel was studied along a 1.6 centimeter long crack. The  $\text{SiO}_2$  and  $\text{CaO}$  contents of the gel are plotted in Fig. 6. Moving from the aggregate (distance = 0 mm) to the cement paste, the silicium content shows a general decreasing trend while the calcium content show a general increasing trend. Such trends have been described by many authors (e.g. (10), (11), Regourd et al. (12), Bérubé and Fournier (13)). However, important variations are observed within these trends. It is to notice that when the crack passes through, or close to an aggregate, the silicium content shows a sudden increase, while the calcium content shows a sudden decrease. Some variations, not related to any occurrence of nearby aggregates, are likely corresponding to a coming gel vein.

## DISCUSSION

The close relationships between the rosette-like gels and wollastonite suggest that the gel were formed from this mineral : wollastonite is therefore likely reactive to AAR. Moreover, its chemical composition is very similar to the AAR gel chemical composition, at least for calcium and silicium. It can be seen in the  $\text{SiO}_2$  versus  $\text{CaO}$  diagram that wollastonite plot within the field of the gel (Fig. 5). The destruction of wollastonite will provide calcium and silicium which are the two main component of AAR gel. The presence of gel within some wollastonite minerals argue for such a reaction (Fig. 4).

The wide variation of the gel chemical composition reflects the complexity of the AAR phenomenon. However, some general chemical trends can be defined (decreasing of the silicium content and increasing of the calcium content from the aggregate to the cement paste). These trends, as described in Fig. 6, are not linear but show important variations. The gel chemical composition present a positive correlation between  $\text{SiO}_2$  and  $\text{K}_2\text{O}$  (Fig. 7). The highest potassium contents were observed for  $\text{SiO}_2$  contents of approximately 70 %. It is likely that these highly alkali enriched gels are the most expansive (Wang and Gillott (14)). These authors stated that alkali-silica complexes, as a difference with lime-alkali-silica complexes, have a high affinity for water and are able to sorb water and therefore to show expansion. On the other hand, no correlation exists between  $\text{SiO}_2$  and  $\text{Na}_2\text{O}$ . It means that, if the potassium enrichment is likely related to the gel formation process, the sodium enrichment is related to another phenomenon (for example, addition of  $\text{NaCl}$  coming from the seawater environment). Indeed, the alkalis may come from the cement, the minerals, or the nearby seawater.

In the  $\text{Na}_2\text{O}$  versus  $\text{K}_2\text{O}$  diagram, the AAR gels can be divided into four groups presenting different  $\text{Na}_2\text{O}/\text{K}_2\text{O}$  ratios (Fig. 8). The first group represented by sample 10 is characterized by low sodium contents but high potassium contents ( $\text{Na}_2\text{O}/\text{K}_2\text{O} \approx 0.1$ ). The second group, represented by the rosette-like gel of the sample 10, is characterized by slightly higher sodium

TABLE 1 - EDXA (E) microanalyses of the AAR gels observed in the studied samples

Sample	Na2O	MgO	Al2O3	SiO2	S	Cl	K2O	CaO	FeO	Total	Na2O +K2O
AAR gel											
1 (E)	1,9	0,1	1,6	46,1	0,0	0,1	2,0	47,8	0,4	100,0	3,9
1 (E)	4,2	0,2	1,9	61,3	0,0	0,1	4,4	27,6	0,2	100,0	8,6
2 (E)	1,0	0,2	0,3	51,3	0,0	0,2	0,4	46,7	0,0	100,0	1,4
2 (E)	2,7	4,1	0,5	41,8	0,0	0,1	0,9	49,7	0,1	100,0	3,6
4 (E)	3,0	0,1	0,3	52,7	0,0	0,1	0,6	43,1	0,0	100,0	3,6
4 (E)	3,2	0,2	1,3	57,2	0,0	0,2	1,6	36,4	0,0	100,0	4,8
5 (E)	2,4	0,0	0,0	66,8	0,0	0,1	3,4	27,3	0,1	100,0	5,8
5 (E)	2,9	0,1	0,9	65,1	0,0	0,4	3,5	27,1	0,1	100,0	6,5
5 (E)	3,6	0,0	0,1	70,4	0,0	0,6	4,0	21,3	0,2	100,0	7,6
5 (E)	1,8	4,3	4,6	40,4	0,0	1,1	0,3	46,8	0,8	100,0	2,1
5 (E)	3,4	0,0	0,5	73,5	0,0	0,5	3,8	18,3	0,0	100,0	7,2
5 (E)	2,6	0,2	1,3	50,0	0,0	0,9	1,0	44,0	0,0	100,0	3,6
5 (E)	2,4	0,0	0,0	56,2	0,0	0,7	1,3	39,4	0,0	100,0	3,7
5 (E)	2,5	0,1	0,0	41,1	0,0	0,5	1,7	54,1	0,0	100,0	4,2
5 (E)	2,9	0,0	0,2	61,6	0,0	1,0	2,4	31,9	0,0	100,0	5,3
5 (E)	3,7	0,0	0,0	55,6	0,0	1,9	2,8	36,0	0,1	100,0	6,5
5 (E)	2,7	0,0	0,1	51,6	0,0	0,3	1,4	43,9	0,1	100,0	4,1
5 (E)	2,9	0,0	0,0	49,3	0,0	0,0	2,1	45,8	0,0	100,0	5,0
5 (E)	2,5	0,2	1,0	46,7	0,0	0,1	1,8	47,4	0,4	100,0	4,3
5 (E)	2,2	0,3	0,6	43,1	0,0	0,5	1,5	51,2	0,6	100,0	3,7
5 (E)	3,1	0,3	0,0	58,4	0,0	0,3	3,0	34,9	0,0	100,0	6,1
5 (E)	3,2	0,1	0,2	53,8	0,0	1,2	3,1	38,5	0,0	100,0	6,3
5 (E)	1,5	0,0	0,0	52,5	0,0	0,0	1,0	45,0	0,0	100,0	2,4
5 (E)	1,8	0,0	3,3	48,1	0,0	0,6	1,1	44,9	0,2	100,0	2,9
5 (E)	3,8	0,1	0,0	46,9	0,0	0,7	3,0	45,4	0,1	100,0	6,8
5 (E)	2,8	0,0	0,1	46,4	0,0	0,1	0,7	49,7	0,2	100,0	3,4
5 (E)	2,6	0,5	0,3	47,3	0,0	0,0	2,1	47,2	0,0	100,0	4,7
5 (E)	2,8	0,1	1,0	49,8	0,0	0,7	0,9	44,4	0,3	100,0	3,7
5 (E)	1,8	0,1	3,3	40,9	0,0	0,8	0,6	51,8	0,7	100,0	2,4
5 (E)	2,6	0,5	1,7	51,4	0,0	0,5	2,1	41,1	0,2	100,0	4,7
5 (E)	2,5	0,0	0,0	41,4	0,0	0,7	1,4	54,0	0,0	100,0	3,9
5 (E)	2,2	0,0	0,4	52,2	0,0	1,2	1,0	43,2	0,0	100,0	3,1
7 (E)	8,5	0,3	0,0	68,2	0,0	0,0	4,4	18,6	0,0	100,0	12,9
9 (E)	7,0	0,3	0,9	58,6	0,0	0,0	2,3	30,7	0,3	100,0	9,2
10 (E)	0,3	0,0	0,0	36,3	0,0	0,0	0,0	63,5	0,0	100,0	0,3
10 (E)	0,6	0,5	0,9	71,0	0,0	0,2	8,7	18,1	0,0	100,0	9,3
10 (E)	0,0	0,0	0,0	64,7	0,0	0,0	4,1	31,2	0,0	100,0	4,1
10 (E)	0,8	0,0	0,0	63,3	0,0	0,0	4,0	31,9	0,0	100,0	4,8
10 (E)	0,1	0,0	0,3	63,6	0,0	0,0	4,2	31,9	0,0	100,0	4,2
10 (E)	0,3	0,0	0,0	63,6	0,0	0,0	4,3	31,7	0,1	100,0	4,6
10 (E)	0,1	0,1	0,0	64,4	0,0	0,1	3,9	31,2	0,1	100,0	4,1
10 (E)	0,0	0,0	0,0	64,0	0,0	0,0	3,9	32,1	0,0	100,0	3,9
10 (E)	0,4	0,2	0,6	57,2	0,0	0,0	2,5	39,2	0,0	100,0	2,9
10 (E)	0,6	0,1	0,4	56,5	0,0	0,0	1,2	41,2	0,0	100,0	1,8
10 (E)	0,2	0,0	0,0	64,3	0,0	0,0	4,1	31,3	0,0	100,0	4,3
10 (E)	0,0	0,1	0,1	64,9	0,0	0,0	3,7	31,2	0,1	100,0	3,7
10 (E)	0,8	0,2	0,0	63,9	0,0	0,0	4,0	31,2	0,0	100,0	4,8
10 (E)	0,5	0,0	0,8	51,1	0,0	0,3	1,3	46,1	0,0	100,1	1,8
10 (E)	0,1	0,3	0,0	64,4	0,0	0,2	4,2	30,8	0,0	100,0	4,3

TABLE 2 - EDXA (E) and microprobe (M) analyses of AAR gel, cement paste & aggregates

Sample	Na2O	MgO	Al2O3	SiO2	S	Cl	K2O	CaO	FeO	Total	Na2O +K2O
10 (M)	0,0	0,0	0,0	63,0	0,0	0,0	6,1	30,8	0,1	100,0	6,1
10 (M)	0,1	0,2	0,0	64,7	0,0	0,0	5,4	29,6	0,0	100,0	5,5
10 (M)	0,0	0,0	0,1	64,0	0,0	0,0	5,7	30,1	0,2	100,0	5,7
10 (E)	0,5	0,0	0,1	30,9	0,0	0,0	0,0	68,5	0,0	100,0	0,5
10 (E)	0,1	0,3	0,0	49,2	0,0	0,1	0,0	50,4	0,0	100,0	0,1
11 (E)	3,7	0,2	1,6	45,6	0,0	0,1	3,2	45,5	0,1	100,0	6,9
11 (E)	4,7	0,0	0,0	45,4	0,0	0,0	2,1	47,8	0,0	100,0	6,8
11 (E)	4,9	0,4	0,9	42,4	0,0	0,3	1,8	49,3	0,1	100,0	6,6
11 (E)	3,3	0,0	0,2	55,4	0,0	0,0	3,1	38,0	0,0	100,0	6,5
AAR rosette-gel											
10 (M)	2,1	2,8	0,4	69,3	0,0	0,0	5,2	20,1	0,2	100,0	7,3
10 (M)	2,8	0,6	1,1	68,7	0,0	0,0	8,2	18,4	0,2	100,0	11,0
10 (M)	2,2	1,8	0,3	68,5	0,0	0,0	10,9	16,2	0,1	100,0	13,1
Calcite											
5 (E)	0,3	0,0	0,9	1,6	0,0	0,5	0,4	96,2	0,1	100,0	0,7
6 (E)	0,3	0,9	3,2	5,0	0,3	0,1	0,0	90,2	0,0	100,0	0,3
10 (M)	0,2	0,0	0,3	6,1	0,0	0,0	0,1	93,4	0,1	100,0	0,2
10 (M)	0,2	1,2	0,2	4,6	0,0	0,0	0,1	93,8	0,0	100,0	0,3
10 (M)	0,4	0,1	0,0	0,0	0,0	0,0	0,1	99,4	0,0	100,0	0,5
Ettringite											
7 (M)	0,1	1,1	14,7	0,5	19,5	0,0	0,0	62,9	1,1	100,0	0,1
Cement paste											
2 (E)	0,0	0,5	0,4	14,1	2,6	0,7	0,2	81,4	0,2	100,0	0,2
5 (E)	1,0	1,9	7,3	27,1	0,0	0,8	0,5	58,1	3,3	100,0	1,5
5 (E)	0,3	1,0	6,0	19,7	0,0	0,2	0,5	72,3	0,0	100,0	0,9
5 (E)	0,6	5,7	0,5	16,7	0,4	0,8	0,6	74,7	0,0	100,0	1,2
5 (E)	1,0	0,2	2,2	35,7	0,0	0,3	0,4	59,8	0,4	100,0	1,4
5 (E)	0,9	0,4	1,8	31,0	0,3	1,8	0,1	63,6	0,2	100,0	1,0
5 (E)	2,1	0,0	3,5	45,7	0,0	0,0	0,3	48,4	0,2	100,0	2,4
5 (E)	1,8	4,5	4,9	48,6	0,0	0,0	0,5	39,3	0,4	100,0	2,4
7 (M)	2,2	0,9	2,6	14,3	0,1	0,0	1,1	78,2	0,7	100,0	3,3
7 (M)	0,5	2,9	3,4	32,0	1,9	0,0	0,0	57,2	2,1	100,0	0,5
11 (E)	1,3	0,0	0,1	20,2	0,0	0,1	0,3	78,0	0,0	100,0	1,6
Wollastonite											
10 (M)	0,0	0,0	0,0	51,2	0,0	0,0	0,0	48,7	0,0	100,0	0,0
10 (M)	0,0	0,1	0,0	51,6	0,0	0,0	0,0	48,2	0,0	100,0	0,0
Plagioclase											
3 (E)	2,9	0,0	26,1	55,8	0,0	0,0	0,7	14,5	0,0	100,0	3,6
5 (E)	3,3	0,0	26,6	53,7	0,0	0,1	0,5	15,9	0,0	100,0	3,8
10 (M)	3,1	0,1	30,7	49,6	0,0	0,0	0,1	15,4	1,0	100,0	3,2
10 (M)	2,9	0,1	30,7	50,1	0,0	0,0	0,1	15,5	0,7	100,0	3,0
10 (M)	5,5	0,0	28,3	55,3	0,0	0,0	0,3	10,5	0,2	100,0	5,7
10 (M)	6,0	0,0	27,1	56,6	0,0	0,0	0,3	9,7	0,3	100,0	6,3
Amphibole											
10 (M)	0,1	16,8	0,3	54,8	0,0	0,0	0,0	26,3	1,8	100,0	0,1
10 (M)	0,2	22,6	2,0	53,3	0,0	0,0	0,0	12,1	9,7	100,0	0,2
10 (M)	1,3	17,2	1,8	53,8	0,0	0,0	0,1	13,8	12,0	100,0	1,4
10 (M)	2,6	15,7	15,1	43,8	0,0	0,0	0,4	12,9	9,4	100,0	3,0
10 (M)	1,3	13,9	13,8	49,7	0,0	0,0	0,0	13,3	8,1	100,0	1,3
10 (M)	1,4	14,2	10,4	52,9	0,0	0,0	0,0	13,0	8,1	100,0	1,5

contents ( $\text{Na}_2\text{O}/\text{K}_2\text{O} \approx 0.2$ ). The third group, represented by the gels of sample 1 and 5, is characterized by similar  $\text{Na}_2\text{O}$  and  $\text{K}_2\text{O}$  contents ( $\text{Na}_2\text{O}/\text{K}_2\text{O} \approx 1$ ). The last group, represented by sample 2, 4, 7, 9, and 11, is characterized by sodium contents higher than the potassium contents ( $\text{Na}_2\text{O}/\text{K}_2\text{O} \approx 2$ ). The differences in the sodium enrichment in these gels, as stated previously, is not correlated to any other chemical variation. It should be pointed out however, that the samples presenting the highest sodium contents come from the outer part of the concrete located in front of the sea. On the other hand, samples 1 and 5, showing equal sodium and potassium contents, also coming from the concrete located in front of the sea, were sampled in the inner part of the structure. Finally, the samples showing the lowest sodium contents, come from the outer part of the structure located in an area not facing the sea. The positive correlation existing between  $\text{Na}_2\text{O}$  and  $\text{Cl}$  (Table 1 and 2) argue for a seawater origin for sodium. These results show therefore that the gel chemical composition reflects directly the environment conditions.

### CONCLUSIONS

This study enlighten the reactive nature of some metamorphic limestones aggregates to AAR and, in this particular case, the role of wollastonite: all the gels were found within the aggregates containing this mineral or even in this mineral. The AAR was accelerated in the studied structure by the presence of seawater. Most of the degradations were observed in the parts facing the sea. The gel chemical composition reflects the seawater proximity. The gel coming from the outer part of the concrete structure are richer in sodium and chloride than the gel coming from the inner part of the concrete structure or from parts not facing the sea. In this case, AAR but also a chloride attack may cause concrete deteriorations.

### REFERENCES

1. Coull, W. A., 1981 "Characteristics and service records of commonly used South African aggregates", Proceedings of the "5th International Symposium on Alkali-Aggregate Reaction in Concrete", Cape Town, South Africa.
2. Rogers, C. A., 1989 "Alkali-aggregate reactivity in Canada", Proceedings of the "8th International Conference on Alkali-Aggregate Reaction", Kyoto, Japan.
3. Fournier, B. and Bérubé, M. A., 1987 "Investigation of the alkali-reactivity potential of limestone aggregates from the Quebec city area (Canada)", Proceedings of the "7th International Conference on Alkali-Aggregate Reaction", Ottawa, Canada.
4. Fournier, B. and Bérubé, M. A., 1989 "Alkali-reactivity potential of carbonate rocks from the St. Lawrence lowlands (Quebec, Canada)", Proceedings of the "8th International Conference on Alkali-Aggregate Reaction", Kyoto, Japan.
5. Durand, B. and Berard, J., 1987, Mat. & Struct. 20, 39.
6. Regourd-Moranville, M., 1989 "Products of reaction and petrographic examination", Proceedings of "8th International Conference on Alkali-Aggregate Reaction", Kyoto, Japan.
7. Brouxel, M., 1991 "Energy dispersive X-Ray analysis (EDXA) : accuracy and reliability", Proceedings of the "3rd Euroseminar on microscopy applied to building materials", Barcelona, Spain.
8. Govindaraju, K., 1989, Geostand. Newsl. 13, 1.
9. Deer, W. A., Howie, R. A. and Zussman, J., 1966, "An introduction to the rock-forming minerals", Longmans, Green and Co, London, England.
10. Knudsen, K. and Thaulow, N., 1975, Cem. & Conc. Res. 5, 443.
11. Brouxel, M., 1992, Cem. & Conc. Res., in press.
12. Regourd, M., Hornain, H., Mortureux, B. and Poitevin, P., 1981 "The alkali-aggregate reaction. Concrete microstructural evolution", Proceedings of the "5th International Symposium on Alkali-Aggregate Reaction in Concrete", Cape Town, South Africa.
13. Bérubé, M. A. and Fournier, B., 1986, Can. Miner. 24, 271.
14. Wang, H. and Gillott, J. E., 1991, Cem. & Conc. Res. 21, 647.

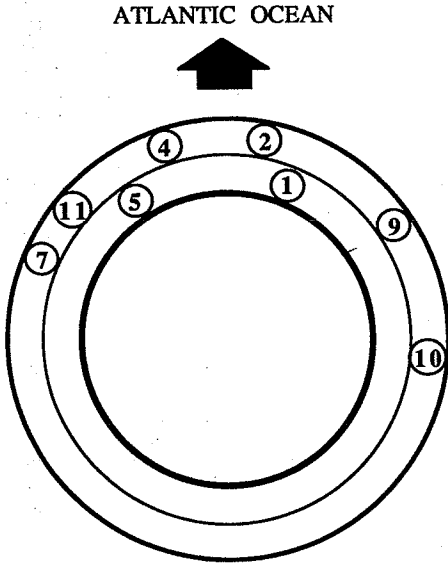


Figure 1 Position of the samples in the inner and outer parts of the tank

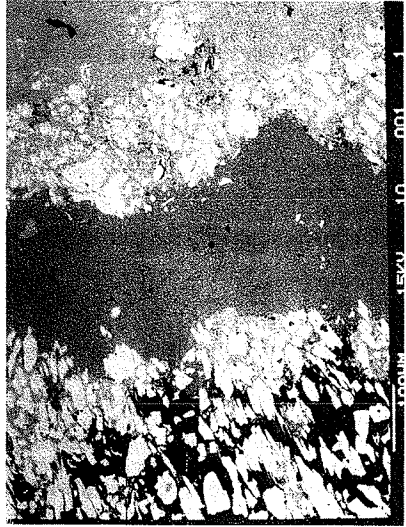


Figure 2 SEM micrograph. See Fig. 3 & 4 for explanations



Figure 3 SEM micrograph (zoom of Fig. 2). Dark gray: gel vein, pale gray: calcite, white minerals: wollastonite, black: rosette-like gel



Figure 4 SEM micrograph (zoom of Fig. 3). Dark gray: gel vein, pale gray: calcite, white minerals: wollastonite, black: rosette-like gel

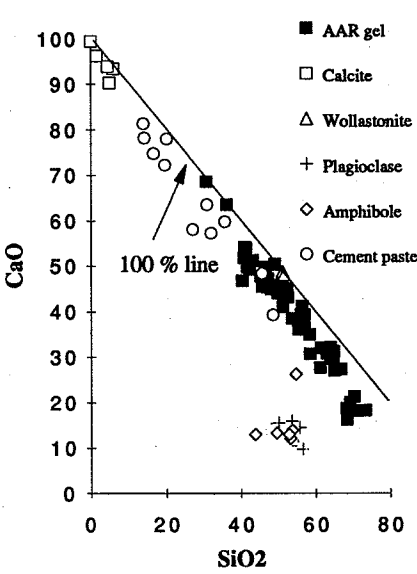


Figure 5 SiO<sub>2</sub> vs CaO graph

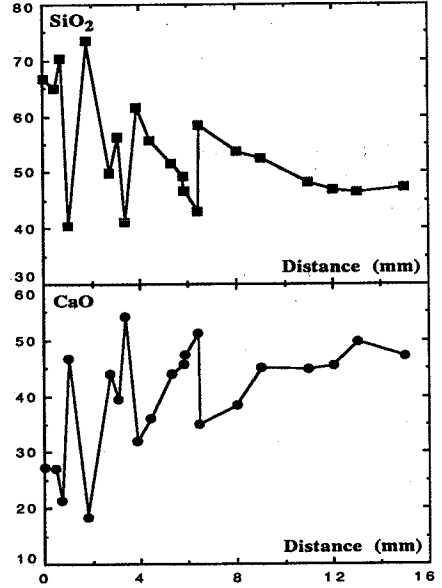


Figure 6 SiO<sub>2</sub> and CaO vs distance from the beginning of a gel vein

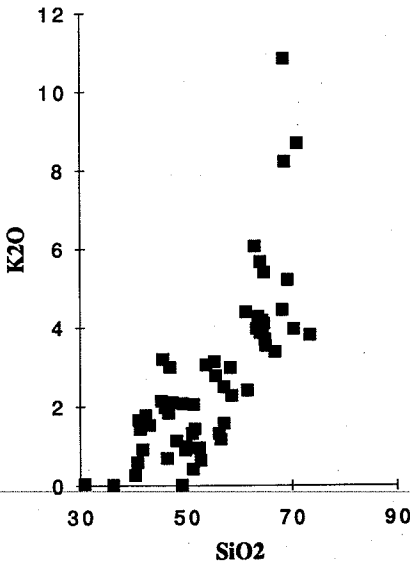


Figure 7 SiO<sub>2</sub> vs K<sub>2</sub>O in the AAR gels

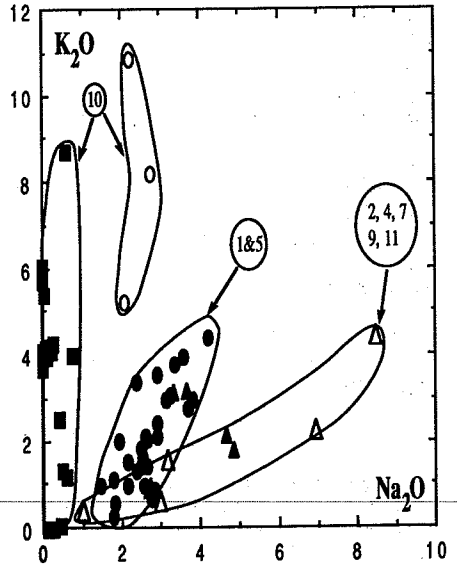


Figure 8 Na<sub>2</sub>O vs K<sub>2</sub>O in the AAR gels. The numbers indicate the sample numbers